Eur Biophys J (2002) 30: 612–616
DOI 10.1007/s00249-001-0191-1

ARTICLE

**Jagannathan Ramesh · Shmuel Argov · Ahmad Salman
Marina Yuzhelevski · Igor Sinelnikov · Jed Goldstein
Vitaly Erukhimovitch · Shaul Mordechai**

Spectroscopic evidence for site-specific cellular activity in the tubular gland in human intestine

Received: 14 June 2001 / Revised: 3 September 2001 / Accepted: 13 September 2001 / Published online: 1 November 2001

Abstract The intestinal crypts contain mucus-secreting goblet cells in large numbers. In the tubular gland (crypt), the cells are generated at the bottom and end their life cycle at the top. Recently, FTIR microspectroscopy (FTIR-MC) has been applied in biology and medicine. The characterization of various cellular types using FTIR-MC and its subsequent application for the diagnosis of cancer is becoming a reality. In this report, we investigate the differential cellular activity in the normal tubular gland using FTIR-MC. Our results indicate that the absorbance for the cells in the bottom of the crypt is always higher than those in the upper portion. There are spectral pattern changes and frequency shifts for cells at the bottom and top sites of the normal crypt. Also, the comparison of a normal crypt with a malignant one has been made. This is the first spectroscopic evidence in the literature showing the difference in the cellular activity at different sites in the tubular gland. The reasons for our observations and their implications are discussed.

Keywords Colon · Cancer · Crypt epithelial cells · FTIR microspectroscopy

Introduction

The human small intestinal surface consists of small crypts having epithelial cells secreting mucosa at the rate of about three litres per day. These secretions contain digestive enzymes, namely proteases, carbohydrate and lipid metabolizing functions (Guyton 1971; Fenogolio-Preiser and Noffsinger 1999). The cells in the normal crypt have a large turnover with a life cycle of approximately 48 hours. The epithelial cells in the normal crypt continuously undergo mitosis at the bottom of the crypt and move gradually along the basement membrane upward and are finally disposed into the intestinal secretions (Potten and Loeffler 1987; Ko et al. 1997; Roncucci et al. 2000). It is speculated that the direction of migration of the cells is reversed in the adenomatous crypt (Roncucci et al. 1993).

Infrared radiation, which is noninvasive and harmless, is absorbed by the tissues, fluids and cells to promote vibration of the covalent bonds of molecules within the sample. The wavelength of the infrared radiation (Mantsch and Chapman 1996) which is absorbed depends upon the nature of the covalent bond (i.e., atoms involved and the type of bond) and the strength of any intermolecular interactions (van der Waals interactions, H-bonding). The IR spectrum of the biological sample is therefore a biochemical fingerprint. Data collection on cells using conventional FTIR spectrometers leads to inaccuracy and loss of sensitivity. This problem has been overcome by the innovation of combining light microscopy with FTIR spectrometers, popularly known as microscopic FTIR (IR Scope). With this advancement in instrumentation, application of FTIR in medicine has become a reality. Myocardial infarction (MI), which accounts for 50% of all deaths in North America, can be detected using the principles of optical biopsy. Based upon the spectral changes for collagen in the heart muscle, MI can be detected quickly where other methods are relatively time consuming and imprecise (Lui et al. 1996). Also, FTIR microspectroscopy (FTIR-MC) has been successfully applied in the characterization of cells (Ramesh et al. 2001a) and consequently in cancer diagnosis (Fabian et al. 1995; Sukuta and Bruch 1999; Rigas et al. 2000; Ramesh et al. 2001b; Salman et al. 2001).

J. Ramesh · A. Salman · M. Yuzhelevski · S. Mordechai (✉)
Department of Physics, Ben-Gurion University,
Beer-Sheva 84105, Israel
E-mail: shaulm@bgumail.bgu.ac.il
Fax: +972-8-6472904

S. Argov · I. Sinelnikov · J. Goldstein
Department of Pathology,
Soroka University Medical Center,
Beer-Sheva 84105, Israel

V. Erukhimovitch
The Institute for Applied Biosciences,
Ben-Gurion University, Beer-Sheva 84105, Israel

To date, there is no spectroscopic investigation on cellular activity in the human crypt in the intestine. In this article, we provide microscopic FTIR proof for the variation in the cellular activity at different sites in the human crypt foci in the intestine. Our results suggest that remarkable differences in the spectra are observed for the cells at the bottom and top of the crypt. Also, the impact of our results is discussed in relevance to cancer diagnosis.

Materials and methods

Sample preparation

Formalin-fixed, paraffin-embedded tissue from which 11 crypts were retrieved from the histopathology files of Soroka University Medical Center, Beer Sheva (SUMC). The tissue samples used in this study were selected to include normal cells located in the crypts. Two paraffin sections were cut from each case: one was placed on a zinc-selenium slide and the other on a glass slide. The thickness of all tissue samples was 10 μm. The first slide was deparaffinized using xylol and alcohol and was used for FTIR measurements. The second slide was stained with hematoxylin and eosin for histology review.

FTIR microspectroscopy

For measurements in transmission mode, we used an FTIR microscope with a liquid nitrogen cooled MCT detector which was coupled to the FTIR spectrometer (Bruker Equinox model 55/S, OPUS software). A pathologist examined each site using combined optical microscopy under standard histological conditions after staining. Each site in the normal and cancer crypts was carefully examined and then the measurements were made. During each measurement, the measured areas of the samples were typically of 100 μm diameter. The measured spectra cover the wavenumber range 600–4000 cm^{-1} in the mid-IR region. The spectra were taken as averages of 128 scans to increase the signal-to-noise ratio. The spectral resolution was 4 cm^{-1}. The baseline was corrected as follows. Initially, the spectrum was divided into 64 sections of equal size. Then the *y*-value minima of the spectrum were connected, generating a curve which gave the best fit to the background. The spectrum was normalized to the amide I peak at 1646 cm^{-1} after baseline correction for the entire spectrum. The error bar (standard error) was calculated for each sample separately for both top and bottom sites of the crypt reported in this article.

Results

Figure 1 shows the FTIR-MC spectra of normal crypts from two different patients. The absorbance for the cells at the bottom (thick lines) site was higher than the top (dotted lines). The absorbance differences between two different crypts for both bottom and top sites were small and hence there was good agreement between various patients. Notable pattern changes were also observed between the bottom and top sites. The cells at the bottom showed a doublet structure pattern between 1000 and 1100 cm^{-1} which was absent for the cells at the upper portion of the crypt. This was observed in all the patients. Doublet frequencies were at 1071 and 1048 cm^{-1} in the given spectrum. The ionized PO_2^- and ribose groups exhibit three vibrations at 1071, 1084 and

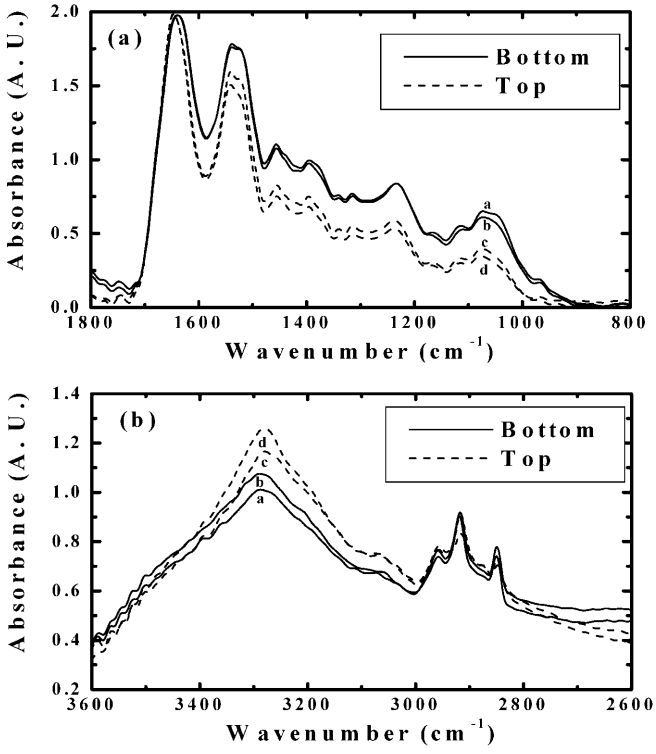

Fig. 1 FTIR microspectroscopy of epithelial cells at the botom (*a*, *b*) and top (*c*, *d*) of a normal crypt in the regions **a** 800–1800 cm^{-1} and **b** 2600–3600 cm^{-1}. This sample was obtained from a younger patient having an advanced stage of the malignancy. Amide I normalization was applied to the spectra shown in this figure

1095 cm^{-1} pertaining to DNA (Diem et al. 1999). The bands at 1025 and 1045 cm^{-1} in IR spectra are assigned to the vibrational modes of -CH_2OH groups as well as the C-O stretching coupled with the C-O bending of the C-OH groups of carbohydrates (includes glucose, fructose and glycogen, etc.) (Parker 1971). Hence the peaks in the doublet are due to symmetric stretching vibrations of the phosphate group from DNA and the stretching and bending modes of the C-O group of carbohydrates. There was a frequency shift of 4–5 cm^{-1} in the amide I peak between the two sites for the younger (47 years) patient whose grading of malignancy was declared as advanced by the pathologist. This can be clearly seen in the second-derivative spectrum shown in Fig. 2. These frequency shifts were observed in another older patient also having an advanced stage of malignancy. The frequency shifts were observed also for amide II, but they were not significant. FTIR-MC spectra in the range between 2600–3600 cm^{-1} showed no significant changes in the absorbance between the two sites. The region beyond 3000 cm^{-1} is not considered for analysis since the absorption is due to traces of water which arise from the intense O-H stretching vibrations which occur between 3000 and 4000 cm^{-1}. To ensure that our results are independent of the methods of treating the spectra, we employed vector normalization to all the spectra (Bruker 1998). The vector normalized spectra are presented in Fig. 3. As can be seen, the absorbance for cells

at the bottom was again higher than the top portion of the normal crypt. The spectral pattern changes, including the hump near 1000 cm^{-1}, could be observed in the spectra from both the top and bottom of the crypt using amide I and vector normalization methods.

Figure 4 shows the FTIR-MC spectra of the bottom portion of normal and malignant crypts from two patients. The absorbance was higher for normal cells compared to the malignant type. Interestingly, the absorbance differences for the amide II band were not significant, as was observed with various sites in the normal crypt. Also, the doublet in the region between 1000 and 1100 cm^{-1} was not observed for the malignant cells. The significant absorbance differences were found only between 1000 and 1500 cm^{-1}, which accounts for the vital metabolites of the cells (Jackson et al. 1997).

The phosphate content derived by integrating the area under the symmetric (1000–1150 cm^{-1}) and asymmetric (1170–1310 cm^{-1}) regions of the phosphate group is presented in Fig. 5a. Our results showed that the phosphate content of the bottom site of the crypt was higher than the top in most of the measurements. The difference in phosphate content between the bottom and top was higher for younger patients (crypt nos. 1–2 and 9–11) relative to older ones. Among them, the difference was largest for the younger patient having an advanced stage of malignancy. Compared to this patient, the difference was lower for the younger patients at a moderate stage of malignancy. However, in older patients the difference in phosphate content was not significant, irrespective of the grade of the malignancy. Several reports suggest that the amide I/II intensity ratio

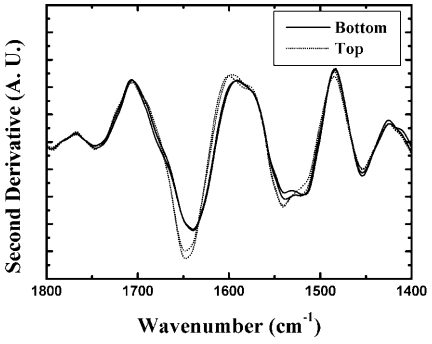

Fig. 2 Second derivative spectra for the sample shown in Fig. 1

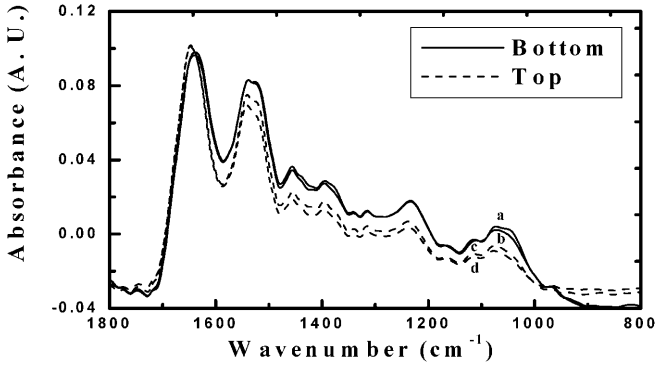

Fig. 3 FTIR-MC spectra shown in Fig. 1 but with vector normalization

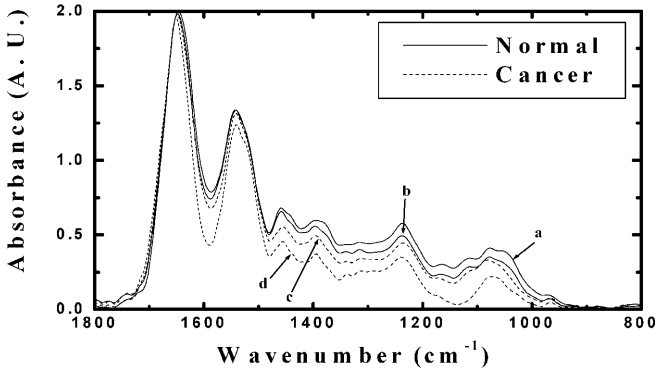

Fig. 4 FTIR-MC spectra of epithelial cells at the bottom of normal (*a*, *b*) and malignant (*c*, *d*) crypts from a patient in the region 800–1800 cm^{-1}

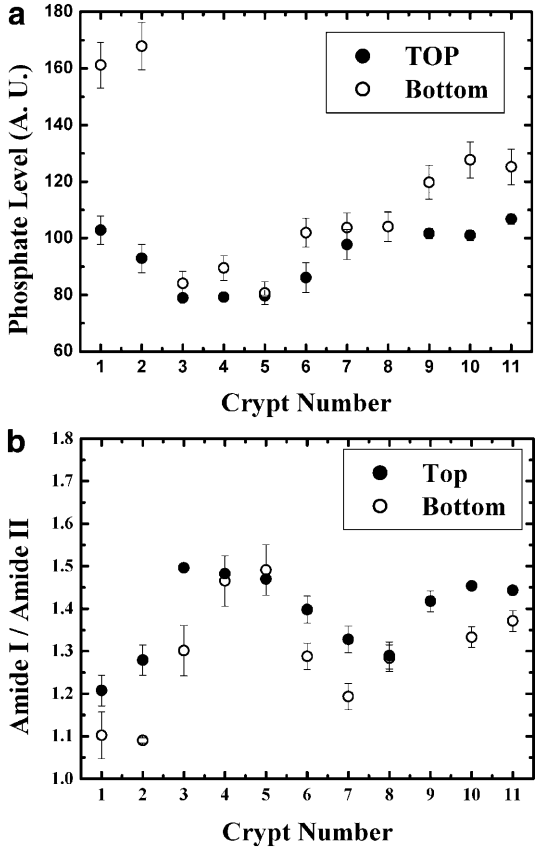

Fig. 5 **a** The phosphate content of epithelial cells at the bottom and top of normal crypts obtained from four patients. The phosphate content was calculated as the sum of the symmetric and asymmetric stretching vibration modes of the phosphate group. OPUS software was for this purpose. **b** Amide I/II ratio as an indicator of DNA content in the cells. The integrated area under the absorption peaks of amide I and II were calculated after baseline correction and amide I normalization

increases with the DNA content of epithelial cells (Benedetti et al. 1997), whereas in the case of red blood cells (RBC) the intensity of the amide I/II ratio is nearly the same as any other pure protein spectrum. The light transmitted during measurement is inversely proportional to the packing density of the nucleus and can be seen as the variation of the amide I/II ratio (Chiriboga et al. 1998). The ratio of the area under amide I/II is shown in Fig. 5b. The results indicated that the cells at the top of the crypt had a higher DNA absorption contribution to the amide I band than those at the bottom. To confirm the above results, we performed a fitting procedure for all the spectra and derived the analytical area for the phosphate and amide I regions. The results (not shown) were in good agreement with the above procedure. The correlation between these two metabolites was found for all the samples in this study.

Discussion

The absorbance differences between the bottom and top sites can be understood from the cellular life cycle in the normal crypt of the human intestine. Generally, in the normal crypt, the epithelial cells are generated in the bottom portion, move upward with differentiation and finally exit, ending up in apoptosis. The recent model (schematically shown in Fig. 6) on histogenesis of colonic adenomas given by Moss et al. (1996) claims that, in adenomas, the proliferation of cells is predominant at the lumen (top of the crypt) and apoptosis at the base (bottom of the crypt), a complete reversal of the normal pattern. The concentration of various metabolites is higher in the cells from the bottom site compared to the top of the crypt and accounts for the absorbance changes between these two sites. This is the reason that the absorbance differences between the bottom and top of the crypt is reflected in the entire region of the spectrum and may be due to the higher metabolic rate of the rapidly growing cells in the bottom relative to the ones undergoing apoptosis at the top of the crypt. This also explains the intensity differences between normal and malignant cells from the bottom of the crypt (Fig. 4). The pattern change in the phosphate region is a useful indicator of any deviation from the normal growth status of the cell (Hoi-Ying et al. 2000). This has been observed also in malignant cells from the human intestine. The frequency shifts observed for amide I and II between the bottom and top sites of the crypts was highest for the younger patient who had an advanced stage of colon cancer. The extent of frequency shifts was in the following order: younger and advanced > older and advanced > younger and moderate > older and moderate. There is a clear trend with age and grade of the malignancy. Probably the conformations associated with some of the proteins would account for these frequency shifts.

The calculation of metabolites such as phosphate and amide I/II content provided some interesting insights. The difference in phosphate content between the bottom and top of the crypt was largest in the younger patient having an advanced stage of malignancy. The process of necrosis (Trump et al. 1997) leading to decreased nuclear density may be the probable reason for this observed difference in absorbance between the top and bottom sites of the crypt. The "younger and moderate" patients also showed a marked difference between the bottom and top sites of the crypt. Other older patients did not show significant changes. The difference in amide I/II was significant for younger patients (both advanced and moderate) and also for the older patient who was in the advanced stage of malignancy.

Our results clearly indicate that both age and the grade of malignancy are the key factors affecting the epithelial cellular activity in the normal crypt, leading to the observed variations in the FTIR spectra. It is important to note that the microscopic FTIR spectra of the normal crypt at different sites can provide valuable information. In particular, the early onset of colon cancer is mainly attributed to genetic reasons (Bonaiti-Pellie 1999; Verma et al. 1999). The limited study reported here shows the power of FTIR-MC in understanding the various factors to be considered in the early diagnosis of malignancy using optical biopsy. More extensive studies

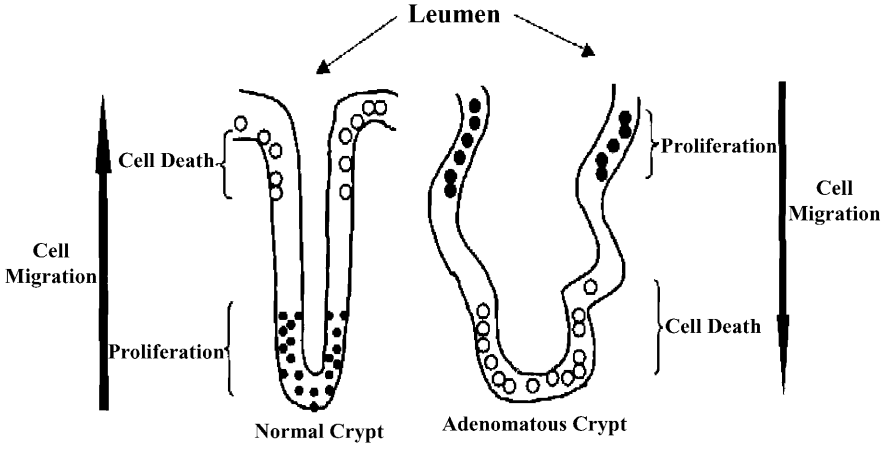

Fig. 6 Schematic representation of a normal (*left*) and adenomatous crypt (*right*) showing cell migration and its corresponding living status. *Filled* and *open circles* represent the cells in exponentially growing and apoptotic stages, respectively

using FTIR-MC may give rise to a novel tool for clinical diagnosis of familial cases with good accuracy.

Conclusions

The human intestine is made up of micro-structures called crypts containing epithelial cells. It is U-shaped where the cells are generated at the bottom, which then move upward and are finally shed into the lumen. In our studies, we have collected FTIR-MC spectra of cells at the bottom and top of normal crypts from the biopsies of colon cancer patients. The absorbance due to the cells at the bottom was higher than at the top site of the crypt in all cases. The higher metabolic rate of the rapidly growing cells accounts for this observation. There were significant pattern changes and frequency shifts observed between cells at the top and bottom of the crypt. The cells at the bottom of a normal crypt showed higher absorbance than the malignant crypt. The histogenesis of normal and malignant cells is the reason for these differences in the absorbance. Our results on biological markers derived from the spectra showed that there was a large difference between the bottom and top of the crypt for a younger patient who had an advanced stage of malignancy. Age and grading of the malignancy are the key factors affecting the FTIR spectral parameters of the normal crypt. Our study may lead to a new path in the diagnosis of colon cancer due to genetic reasons.

Acknowledgements This research work was supported in part by the Middle East Cancer Consortium (MECC), the Cancer Research Foundation at the Soroka University Medical Center in Memory of Prof. Tabb and the Harry Stern Applied Research Grant program. Fruitful discussions with Dr. B. Cohen are gratefully acknowledged.

References

Benedetti E, Bramanti E, Papineschi F, Rossi I (1997) Determination of the relative amount of nucleic acids and proteins in leukemic and normal lymphocytes by means of FT-IR microspectroscopy. Appl Spectrosc 51:792–797

Bonaiti-Pellie C (1999) Genetic risk factors in colorectal cancer. Eur J Cancer Prev 8:S27–S32

Bruker (1998) OPUS NT version 1.0 reference manual. Bruker, Germany, p 71

Chiriboga L, Xie P, Yee H, Zarou D, Zakim D, Diem M (1998) Infrared spectroscopy of human tissue. IV. Detection of dysplastic and neoplastic changes of human cervical tissue via infrared microscopy Cell Mol Biol 44:219–229

Diem M, Boydston-White S, Chiriboga L (1999) Infrared spectroscopy of cells and tissues: shining light onto a novel subject. Appl Spectrosc 53:148–161

Fabian H, Jackson M, Murphy L, Watson PH, Fichtner I, Mantsch HH (1995) A comparative infrared spectroscopic study of human breast tumors and breast tumor cell xenografts. Biospectroscopy 1:37–45

Fenogolio-Preiser CM, Noffsinger A (1999) Aberrant crypt foci: a review. Toxicol Pathol 27:632–642

Guyton AC (1971) Medical physiology. Saunders, Philadelphia, chap 64

Hoi-Ying NH, Goth-Goldstein R, Eleanor AB, Kathy B, Micheal CM, Wayne RM (2000) Individual human cell responses to low doses of chemicals studied by synchrotron infrared spectromicroscopy. SPIE 3918:57–63

Jackson M, Sowa MG, Mantsch HH (1997) Infrared spectroscopy: a new frontier in medicine. Biophys Chem 68:109–125

Ko TC, Bresnahan WA, Thompson EA (1997) Intestinal cell cycle regulation. Prog Cell Cycle 3:43–52

Lui K, Jackson M, Sowa MG, Ju H, Dixon IM, Mantsch HH (1996) Modification of the extracellular matrix following myocardial infarction monitored by FTIR spectroscopy. Biochim Biophys Acta 1315:73–77

Mantsch HH, Chapman D (eds) (1996) Infrared spectroscopy of biomolecules. Wiley, New York, chaps 2, 6–9

Moss SF, Liu TC, Petrotos A, Hsu TN, Gold LI, Holt PR (1996) Inward growth of colonic adenomatous polyps. Gastroenterology 111:1425–1432

Parker FS (1971) Application of infrared spectroscopy in biochemistry, biology and medicine. Plenum, New York

Potten CS, Loeffler M (1987) A comprehensive model of the crypts of the small intestine of the mouse provides insight into the mechanism of cell migration and the proliferation hierarchy. J Theor Biol 127:381–391

Ramesh J, Salman A, Hammody Z, Cohen B, Gopas J, Grossman N, Mordechai S (2001a) FTIR microscopic studies on normal and H-*ras* oncogene transfected cultured mouse fibroblasts. Eur Biophys J 30:250–255

Ramesh J, Salman A, Argov S, Goldstein J, Sinelnikov I, Walfisch S, Guterman H, Mordechai S (2001b) FTIR microscopic studies on mormal, polyp and malignant human colonic tissues. Subsurf Sensing Technol Appl 2:99–117

Rigas B, LaGuardia K, Qiao L, Bhandare PS, Caputo T, Cohenford MA (2000) Infrared spectroscopic study of cervical smears in patients with HIV: implications for cervical carcinogenesis. J Lab Clin Med 135:26–31

Roncucci L, Pedroni M, Fante R, Di Gregorio C, Ponz de Leon M (1993) Cell kinetic evaluation of human colonic aberrant crypts. Cancer Res 53:3726–3729

Roncucci L, Pedroni M, Vaccina F, Benatti P, Marzona L, De Pol A (2000) Aberrant crypt foci in colorectal carcinogenesis: cell and crypt dynamics. Cell Prolif 33:1–18

Salman A, Argov S, Ramesh J, Goldstein J, Igor S, Guterman H, Shaul M (2001) FTIR microscopic characterization of normal and malignant human colonic tissues. Cell Mol Biol 47:159–166

Sukuta S, Bruch R (1999) Factor analysis of cancer Fourier transform infrared evanescent wave fiberoptical (FTIR-FEW) spectra. Lasers Surg Med 24:382–388

Trump BF, Berezesky IK, Chang SH, Phelps PC (1997) The pathways of cell death: oncosis, apoptosis, and necrosis. Toxicol Pathol 25:82–88

Verma L, Kane MF, Brassett C, Schmeits J, Evans DG, Kolodner RD, Maher ER (1999) Mononucleotide microsatellite instability and germline MSH6 mutation analysis in early onset colorectal cancer. J Med Genet 36:678–682